Available online at www.sciencedirect.com
ScienceDirect
Trans. Nonferrous Met. Soc. China 21(2011) 1957−1962
Transactions of Nonferrous Metals Society of China
www.tnmsc.cn

Effect of pre-stretching on microstructure of aged 2524 aluminium alloy

QUAN Li-wei[1, 2], ZHAO Gang[1], Sam GAO[2], Barry C. MUDDLE[2]

1. School of Materials and Metallurgy, Northeastern University, Shenyang 110004, China;
2. ARC Centre of Excellence for Design in Light Metals, Monash University, Victoria 3168, Australia

Received 30 October 2010; accepted 27 May 2011

Abstract: The effects of pre-stretching following solution treatment on the hardness and microstructures of aged 2524 aluminium alloy at 170 °C were studied. Ageing hardness values under different pre-stretching conditions were measured, and the corresponding microstructures were characterized by transmission electron microscopy (TEM). The results show that compared with unstretched samples, the peak hardness is increased and the time to reach the peak hardness is reduced with the increase of pre-strain; the number density of *S* (Al_2CuMg) phases is increased and the length is shortened in pre-stretched alloy. Additionally, the number density of GPB zones is decreased with the increase of pre-strain in peak-aged samples. When the pre-strain is up to 5%, *S* phases play the predominant contribution to the peak hardness. Fine and uniformly distributed *S* phases lead to a higher hardness than GPB zones together with *S* phases existing in conventionally aged 2524 alloy.
Key words: 2524 aluminium alloy; pre-stretch; *S* phase; GPB zone

1 Introduction

2524 aluminum alloy is heat treatable and responds to precipitation hardening with GPB zones and *S* phase as the strengthening precipitates. It has been widely used as aerospace material due to its high strength, good damage tolerance and creep resistance. The commercial 2524 alloy is normally solution heat treated, quenched and then artificially aged. After solution treatment, it is necessary to proceed pre-stretching to reduce the residual stress formed in quench with a pre-strain no more than 5%. Therefore, the precipitation characterization may be affected by pre-stretching. It is reported that the coalesce process of *S′* precipitates into corrugated sheets and wide plates does not occur until long-term over-aging in the stretched Al-2.62Cu-1.35Mg alloy and 2024 alloy with a pre-strain of 1.5%. Meanwhile, the nucleation rate and nucleus density for the precipitation of *S′* phases are stimulated by applying a strain [1]. The heterogeneous nucleation sites are increased by pre-stretching, thus refining the *S* precipitates [2]. Nowadays, HUANG et al [3] pointed out that finer and thinner *S″* phase can be obtained in Al-4.45Cu-1.5Mg alloy by cold rolling with a reduction of around 40% followed by ageing. In addition, the effect of pre-stretching on the precipitation process in other alloys is also found [4−6]. At the same time, many people pay attention to the mechanical properties of the alloy with a pre-strain. ZHANG et al [7] and LI et al [8] found that the pre-deformation can increase the strength and decrease the elongation of 2519 alloy. Despite of these reports, there has been no detailed microstructure analysis reported on the mechanism of the effect of pre-stretching on the aged 2524 alloy. The aim of this work is to present the effect of various pre-strains on the ageing hardening response and the corresponding microstructures of the 2524 aluminium alloy.

2 Experimental

The commercial 2524 alloy was used in this study with the chemical compositions listed in Table 1. Tensile specimens punched from as-rolled alloy sheet of 4 mm in thickness were solution treated at 495 °C for 1 h, quenched into water at room-temperature, and then stretched with an Instron machine to different strains of 0, 2% and 5% at room temperature with a strain rate of 1 mm/min. Then the pre-strain specimens were

Foundation item: Project (51001022) supported by the National Natural Science Foundation of China; Project supported by Innovative Research Team in University of Liaoning Province, China
Corresponding author: ZHAO Gang; Tel: +86-24-83681685; Email: zhaog@mail.neu.edu.cn
DOI: 10.1016/S1003-6326(11)60956-4

immediately aged in an oil bath at 170 °C for different ageing time to minimize the natural ageing effect. Vickers hardness measurement was carried out with a load of 49 N and dwell time of 20 s. Thin foils for transmission electron microscopy (TEM) observation were prepared by cutting, grinding and punching into discs of 3 mm, followed by electro-polishing in a twin-jet Tenupol by a 33% nitric acid solution in methanol operated at −25 °C and 13.8 V. Philips CM20 TEM operated at 200 kV was used to observe the microstructures.

Table 1 Chemical composition of commercial 2524 alloy (mass fraction, %)

Si	Fe	Cu	Mn	Mg	Cr	Ni	Zn	Ti	Al
0.03	0.11	4.2	0.62	1.5	0.01	0.01	0.02	0.01	Bal.

3 Results and discussion

3.1 Effect of pre-stretching on hardness

Figure 1 shows the ageing hardness curves of the alloy at 170 °C with different pre-strains of 0, 2% and 5%. It can be seen clearly that the pre-stretching increases ageing hardness values. The initial hardness value immediately measured after quenching is about VHN 97 while it is about VHN 108 and VHN 125 for the samples with pre-strain of 2% and 5%, respectively. This can be ascribed to the work hardening effect, with a larger pre-strain resulting in a higher hardness. When the samples were subsequently aged at 170 °C for 5 min, the hardness values increase significantly to VHN 126, VHN 135 and VHN 139 for samples with the pre-strain of 0, 2% and 5%, respectively. Then the ageing hardness curves are leveled for a period until the second hardening stage starts. The pre-strain can significantly increase the peak hardness and reduce the time to reach peak hardness. The un-stretched sample can reach the peak hardness of VHN 142 at about 72 h. In contrast, the peak hardness values are about VHN 163 and VHN 170 and the times required to achieve the peak hardness are about 47 and 36 h for samples with the pre-strain of 2% and 5%, respectively. As can be seen from Fig. 1, the peak hardness increases with increasing the pre-strain. Meanwhile, it can be also found that the time for attaining peak hardness is reduced due to the pre-stretching.

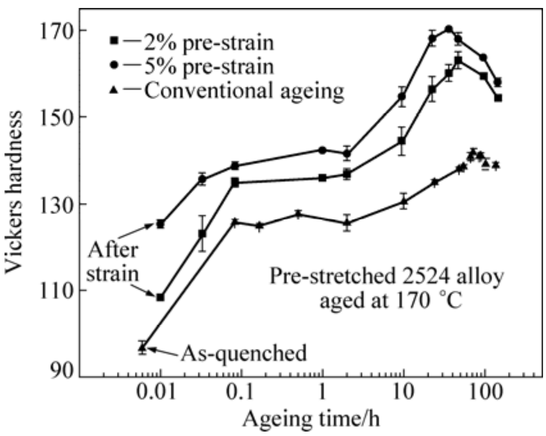

Fig. 1 Ageing hardness curves of alloys with various pre-strains followed by isothermal ageing at 170 °C and load of 49 N

3.2 Effect of pre-stretching on microstructures of alloy

3.2.1 Pre-strain

Figure 2 shows the microstructures of the solution treated, quenched (and then pre-stretched) Al-Cu-Mg alloys. The bright field (BF) TEM micrographs were recorded near the ⟨001⟩ incident beam and corresponding selected area diffraction (SAD) patterns were recorded parallel to $\langle 001\rangle_\alpha$ zone axes with respect to the BF images, which provides a basis for analysis of the precipitate structures. There is no detectable precipitate in as-quenched alloy shown in Fig. 2(a). The corresponding SAD pattern in Fig. 2(d) also reveals that no secondary phase forms in this alloy. However, from Figs. 2(b) and (c), it can be clearly seen that an appreciable number of dislocations are formed due to the pre-strain. Besides dislocation loops, numerous helical dislocations are also present in the pre-stretched alloy. Figure 2(c) contains the highest density of defects in the form of dislocations. The corresponding SAD patterns in Figs. 2(e) and (f) illustrate that no precipitates can be detected in the pre-stretched alloy with 2% or 5% pre-strain, which is responding to the initial hardness in the hardness curves in Fig. 1. It is related to the work hardening which generates many tangled dislocations and thus increases the hardness. Therefore, it can be concluded that the increase of hardness after pre-stretching is attributed to the tangled dislocations inducing work hardening effect on the alloy in the initial ageing stage.

Generally, dislocation loops in Al-Cu-Mg alloy are resulted from the collapse of vacancies generated after quenching and growing with increasing ageing time. Excess vacancies occur in the supersaturate solid solution after quenching and migrate with time going on. Then the vacancies condense and collapse to form dislocation loops on adjacent $\{111\}_\alpha$ plane [9]. They can grow to a large size when quenched alloy is natural-aged at room temperature or artificially aged for a short time. Therefore, the absence of dislocation loops in Fig. 2(a) can be ascribed to the inadequate time to collapse and grow. However, a lot of dislocations generate after pre-stretching. The pre-strain can promote clustering and migration of vacancies to dislocations or surface, which

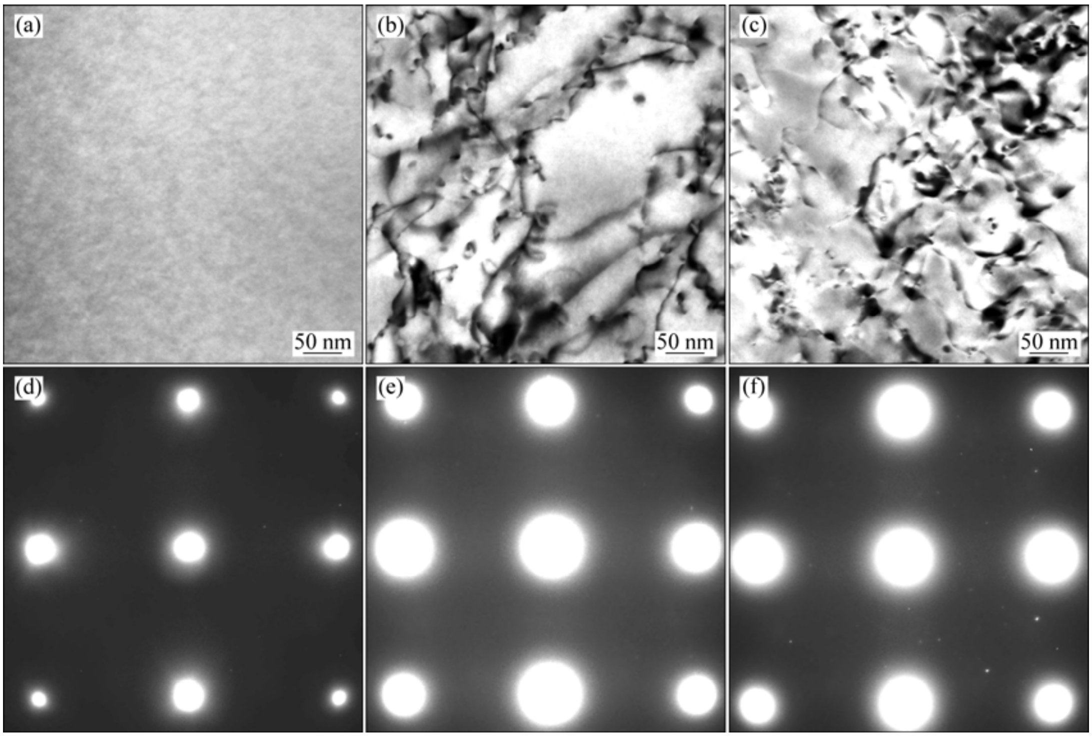

Fig. 2 ⟨001⟩ BF TEM micrographs of alloys with various strains of 0 (a), 2% (b) and 5% (c) and corresponding SAD patterns of pre-stretched samples with various strains of 0 (d), 2% (e) and 5% (f), respectively

results in lots of dislocations and some dislocation loops (Figs. 2(b) and (c)). The larger the strain is, the more the dislocations form. As a consequence, the density of dislocations in 5%-pre-stretched alloy is higher than that in 2% pre-stretched alloy, which is in agreement with the results of other authors [1, 10]. It is generally regarded that the precipitation sequence in Al-Cu-Mg alloy in α+S phases is: SSSS-clusters→GPB zones→GPB zones+S phase→S phase. S phases initially nucleate on the dislocations and grow with the relationship with matrix as $\{100\}_S//\{012\}_{Al}$ including 12 variants [11]. These dislocations will provide enough nucleation sites for the nucleation of S phase.

3.2.2 Underageing

S precipitates prefer to nucleate and grow on dislocations which are increased in number density due to the pre-stretching. These dislocations provide enough nucleation sites for the nucleation and growth of S phase in the later ageing process. With increasing the ageing time to 2 h, S phases nucleate and grow on dislocation loops or helical dislocations in the pre-stretched alloy with a pre-strain of 2%, as shown in Fig. 3(a). These loops lie on {111} planes with large dimension responding to the onset of the second hardening stage. Compared with the SAD pattern in Fig. 2(e), the streaks in SAD pattern in Fig. 3(b) clearly indicate the appearance of S phases. Meanwhile, the BF TEM image also implies that S phases preferentially grow on dislocation lines. So when 2524 alloy is aged at 170 °C

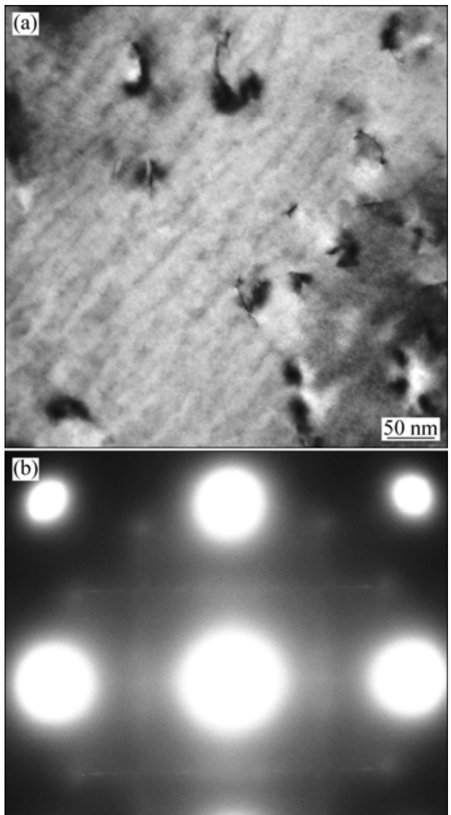

Fig. 3 BF TEM micrograph (a) and corresponding SAD pattern (b) of sample aged for 2 h with strain of 2%

for a short time, S phases believably prefer to nucleate and grow on dislocation lines.

3.2.3 Peak ageing

The $\langle 001\rangle_\alpha$ BF TEM micrographs and the corresponding SAD patterns of the peak-aged microstructures with various pre-strains are provided in Fig. 4. In the peak-aged conditions, S phases exist in both the pre-stretched and unstretched alloys. However, it can be seen clearly that the lengths of the S phases in the 2% (Fig. 4(b)) and 5% (Fig. 4(c)) pre-stretched alloys are about 185 and 66 nm, respectively, which are significantly shorter than that of about 415 nm in the alloy without pre-stretching (Fig. 4(a)). Another interesting feature observed is that there are different S phase distributions. In the 0% and 2% pre-stretched alloys S phases heterogeneously distribute on dislocations, while in the 5% pre-stretched alloy the distribution of the S phases appears to be more uniform throughout the α-matrix. In Fig. 4(c), the length of S phases is significantly shortened and the number density of S phases is increased by pre-stretching.

GPB zones in Al-Cu-Mg alloy are generally considered to have the predominant contribution to the peak hardness [12−15], though some other authors proposed S phases as the strengthening precipitates [14, 16−17]. However, the results present in this work are in agreement with those of RINGER et al [12]. A lot of uniformly distributed GPB zones (marked as arrow in Fig. 4(a)) can be observed in the alloy without pre-strain. As shown in Fig. 4(d) the streaks further confirm the formation of GPB zones [18]. The GPB zones decrease with increasing the pre-strain. There are only a few of GPB zones left in the alloy with 2% pre-strain in Fig. 4(b). And almost no visible GPB zones can be found in the 5% pre-strain alloy in Fig. 4(c). The sharp spots in SAD pattern in Fig. 4(e) reveal the lower density of GPB zones. No streaks of GPB zones can be observed in the SAD pattern (Fig. 4(f)), which is attributed to the S phases as the predominant precipitate under this condition. Figure 5 shows the simulated diffraction pattern of S phases. This is consistent with the experimental diffraction pattern of the matrix and S phases in Fig. 4(f). The simulated diffraction pattern further proves that most of the precipitates in this pre-stretched alloy with 5% pre-strain are S phases.

The dislocations generated in the pre-stretched alloy can provide nucleation sites for the precipitation of S phases. Therefore, the number density of S phases in pre-stretched alloy is larger than that of the alloy without pre-strain. Meanwhile, due to the constant magnesium and copper solute atoms in the matrix, the volume of the precipitation is constant at a certain condition. At the same time the density of S phases is larger, so the dimension of S phase becomes small. As a result the length of S phase is decreased with increasing the pre-strain, which is consistent with results of other

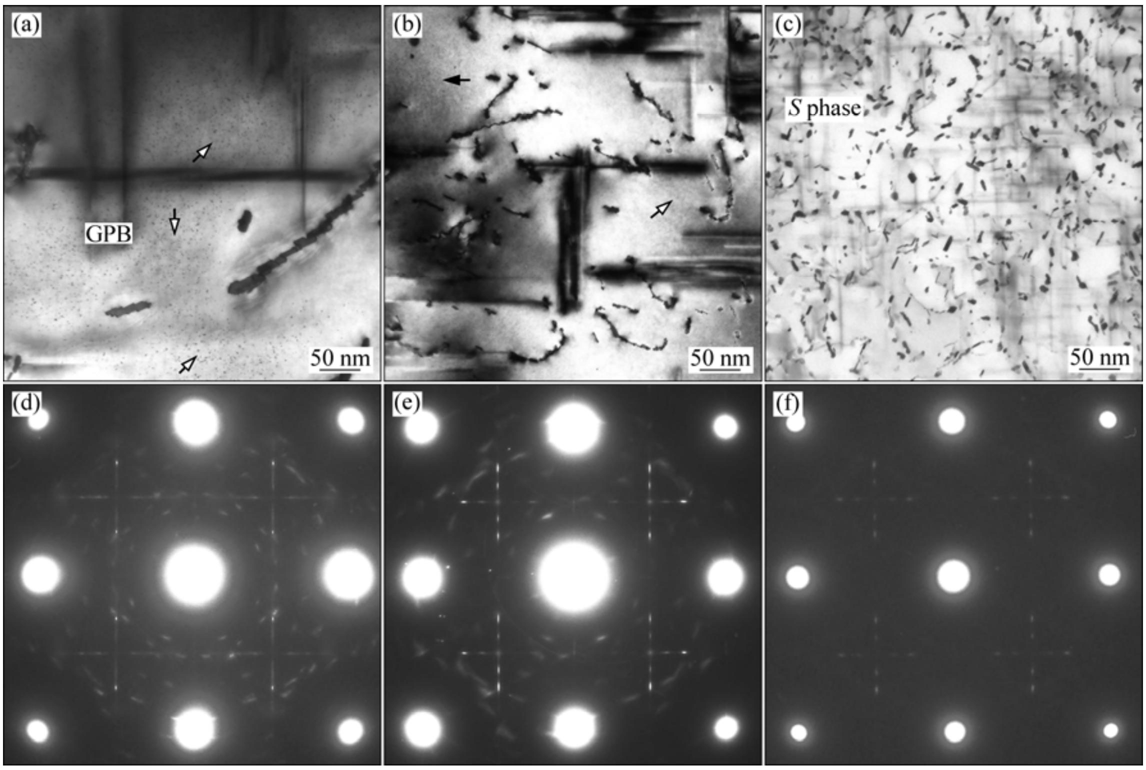

Fig. 4 $\langle 001\rangle_\alpha$ BF TEM micrographs of samples with various strains of 0 (a), 2% (b) and 5% (c) and corresponding SAD patterns of peak-aged samples with various strains of 0 (d), 2% (e) and 5% (f), respectively

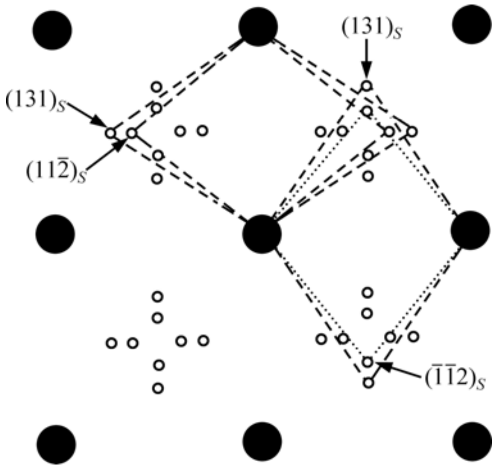

Fig. 5 Simulated diffraction pattern of S phase (●—Al reflections; ○—S phase)

researches [1−3].

When the alloy is conventionally aged to peak hardness, GPB zones are generally considered to have the predominant contribution to the maximum hardness. As shown in Fig. 4(a), there are S phases and lots of GPB zones coexisting in the peak-aged alloy without pre-strain. These S phases are heterogeneously and coarsely distributed in the matrix. The heterogeneous coarse S phases leave wide space for the formation of GPB zones. However, with a pre-strain which promotes the nucleation of S phases, the fine and uniform S phases do not leave enough space for the formation of GPB zones. The dislocations generated from pre-stretching attract the solute atoms to form the S phase, leading to the less concentration residing in matrix. Then the number density of GPB zones is decreased. This could be illustrated as shown in Fig.4 (b) and Fig. 4(c), the number of GPB zones in the alloy with 2% pre-strain is significantly decreased compared with the alloy without pre-strain (Fig. 4(a)), and few GPB zones can be obtained with a pre-strain of 5%. Consequently, the number of GPB zones decreases with increasing the pre-strain. And the fine S phases become the main precipitates in the peak-aged alloy.

4 Conclusions

1) Pre-stretching can result in a higher hardness compared with conventionally aged 2524 alloy. And it can reduce the time to reach peak hardness.

2) Pre-stretching introduces lots of dislocations which provide many nucleation sites for S phases. Therefore the density of S phases is high and the S phases are fine in 2524 alloy.

3) GPB zones have the predominant contribution to the maximum hardness in the conventionally aged sample. But it is the refined S precipitates, with a uniform distribution and high density, which plays a significant role in the peak hardness of the aged alloy with a 5% pre-strain. The microstructure of fine and uniformly distributed S phases leads to a higher hardness than GPB zones together with S phases existing in conventionally aged 2524 alloy.

Acknowledgements

The authors wish to thank Monash Center of Electron Microscopy, Australia, for providing the access of the equipment. The authors also gratefully acknowledge the financial support by Chinese Scholarship Council.

References

[1] SHIH H, HO N, HUANG J C. Precipitation behaviors in Al-Cu-Mg and 2024 aluminum alloys [J]. Metallurgical and Materials Transactions A, 1996, 27: 2479−2494.

[2] WILSON R N, PARTRIDGE P G. The nucleation and growth of S' precipitates in an aluminum-2.5%copper-1.2%magnisium alloy [J]. Acta Metallurgica, 1965, 13: 1321−1327.

[3] HUANG Y J, CHEN Z G, ZHENG Z Q. A conventional thermo-mechanical process of Al-Cu-Mg alloy for increasing ductility while maintaining high strength[J]. Scripta Materialia, 2011, 64: 382−385.

[4] LI Zhou-bing, SHEN Jian, LEI Wen-ping, YAN Liang-ming, LI Jun-peng, MAO Bai-ping. Effects of prestretching on precipitated phase and mechanical properties of Al-Cu-Mg-Ag alloy [J]. The Chinese Journal of Nonferrous Metals, 2010, 20(8): 1508−1512. (in Chinese)

[5] RINGER S P, MUDDLE B C, POLMEAR I J. Effect of cold work on precipitation in Al-Cu-Mg-(Ag) and Al-Cu-Li-(Mg-Ag) alloys [J]. Metallurgical and Materials Transactions A, 1995, 26: 1659−1671.

[6] ÜNLÜ N, GABLE B M, SHIFLET G J, STARKE E A Jr. The effect of cold work on the precipitation of Ω and θ' in a ternary Al-Cu-Mg alloy [J]. Metallurgical and Materials Transactions A, 2003, 34: 2757−2769.

[7] ZHANG Xin-ming, LIU Ling, JIA Yu-zhen. Microstructures and mechanical properties of 2519A aluminum alloy [J]. The Chinese Journal of Nonferrous Metals, 2010, 20(6): 1088−1094. (in Chinese)

[8] LI Hui-zhong, ZHANG Xin-ming, CHEN Ming-an, ZHOU Zhuo-ping, GONG Min-ru. Effect of pre-deformation on microstructures and mechanical properties of 2519 aluminum alloy [J]. The Chinese Journal of Nonferrous Metals, 2004, 14(12): 1990−1994. (in Chinese)

[9] WESTMACOTDT K H, HULL D, BARNES R S. Dislocation sources in quenched aluminium-based alloys [J]. Philosophical Magazine, 1959, 45(4): 1089−1092.

[10] CASSADA W A, SHIFLET G J, STARKE JR E A. The effect of plastic deformation on Al_2CuLi(T1) precipitation [J]. Metallurgical Transaction A, 1991, 22: 299−306.

[11] WANG S C, STARINK M J. Precipitates and intermetallic phases in precipitation hardening Al-Cu-Mg-(Li) based alloys [J]. International Materials Reviews, 2005, 50: 193−215.

[12] RINGER S P, HONO K, POLMEAR I J, SAKURAI T. Nucleation of precipitates in aged Al-Cu-Mg-(Ag) alloys with high Cu:Mg ratios [J]. Acta Materialia, 1996, 44(5): 1883−1898.

[13] RINGER S P, HONO K, SAKURAI T, POLMEAR I J. Cluster

hardening in an aged Al-Cu-Mg alloy [J]. Scripta Materialia, 1997, 36(5): 517−521.

[14] KHAN I N, STARINK M J, YAN J L. A model for precipitation kinetics and strengthening in Al-Cu-Mg alloy [J]. Materials Science and Engineering A, 2008, 472: 66−74.

[15] RINGER S P, SAKURAI T, POLMEAR I J. Origins of hardening in aged Al-Cu-Mg-(Ag) alloys [J]. Acta Materialia, 1997, 45(9): 3731−3744.

[16] STARINK M J, YAN J L. Precipitation hardening in Al-Cu-Mg alloys: analysis of precipitates, modeling of kinetics, strength predictions [J]. Materials Science Forum, 2006, 519−521: 251−258.

[17] WANG S C, STARINK M J, GAO N. Precipitation hardening in Al-Cu-Mg alloys revisited [J]. Scripta Materialia, 2006, 54: 287−291.

[18] KOVARIK L, COURT S A, MILLS M J. GPB zones and composite GPB/GPBII zones in Al-Cu-Mg alloys [J]. Acta Materialia, 2008, 56: 4804−4815.

预拉伸对时效 2524 铝合金微观组织的影响

权力伟[1,2]，赵 刚[1]，Sam GAO[2]，Barry. C. MUDDLE[2]

1. 东北大学 材料与冶金学院，沈阳 110004；

2. ARC Centre of Excellence for Design in Light Metals, Monash University, Victoria 3168, Australia

摘 要：研究了 2524 铝合金在固溶处理后立即预拉伸对随后在 170 °C 时效的硬度和微观组织的影响。测量了在不同预拉伸条件下的时效硬度，并通过透射电镜观察其微观组织。结果表明：与未拉伸样品相比，随着预拉伸量的增加，预拉伸样品的峰值硬度值逐渐增加，而达到峰值硬度所需的时间也逐渐缩短；预拉伸合金中，*S*(Al_2CuMg)相的数量增多，但其长度缩短；此外，峰值状态 GPB 区的密度随着应变量的增加而减小。当预拉伸应变达到 5%时，*S* 相对峰值状态起主要作用。常规时效的 2524 合金在峰值时以 GPB 区和 *S* 相为主，在预拉伸样品中更弥散、细小的 *S* 相导致硬度值高于常规时效的值。

关键词：2524 铝合金；预拉伸；*S* 相；GPB 区

(Edited by LI Xiang-qun)